

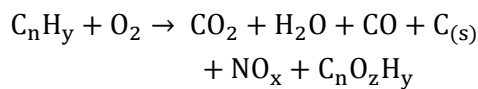
# High-Speed Infrared Imaging for Analysis of a Diesel Engine Supplied with a Premixed Methane-Air Charge

Efforts are continuously made to improve internal combustion engines' (ICEs) efficiency. Lowering fuel consumption and reducing soot formation are among the challenges being addressed when seeking to improve engine designs. In this work, ICE characterization was carried out on an elongated single-cylinder transparent diesel engine equipped with the multi-cylinder head of a commercial passenger's car and a common rail injection system. The engine uses a conventionally extended piston where part of the piston's crown is replaced by a sapphire window. In this configuration, a full view of the combustion bowl can be achieved while the engine is in operation by looking at a 45° fixed mirror located in the extended piston axis. Infrared imaging was carried out at 26 kHz, leading to a temporal resolution of about 0.35° crankshaft angle, at 1500 RPM, in the engine's reference frame. In the experiment, air was replaced by a premixed air-methane charge in order to improve combustion and lower the amount of soot deposits. The different phases of a combustion cycle, i.e. intake, compression, fuel injection, working stroke and exhaust, were investigated using four different spectral filters (broadband, CO<sub>2</sub> red-spike, through-flame and hydrocarbon). The results illustrate the potential of high-speed IR imaging as a diagnostic tool for ICEs.

## Introduction

Internal combustion engines (ICEs) are part of everyday life as they are found in most vehicles around the world. Although the market for hybrid and electric cars is undergoing a sustained growth, the majority of ICEs are still using diesel as their main fuel. In optimal conditions, combustion of hydrocarbon fuel should essentially produce water vapor (H<sub>2</sub>O) and carbon dioxide (CO<sub>2</sub>). Despite all the efforts made by the manufacturers to improve engine designs, fossil fuel (C<sub>n</sub>H<sub>y</sub>) combustion in ICEs still produces considerable amounts of soot particles (C<sub>(s)</sub>) and other pollutants like carbon monoxide (CO), nitrogen oxides (NO<sub>x</sub>) and partially oxidized and/or unburnt hydrocarbons (C<sub>n</sub>O<sub>z</sub>H<sub>y</sub>), as shown in Equation 1.

### Equation 1



Among the strategies used to improve combustion efficiency in compression ignition (CI) engines is the use of multi-injection sequences. In such a case, the use of a

pilot injection helps to ignite the main fuel injection, resulting in less unburnt hydrocarbons and particulate matters in the exhaust gases. However, this does not

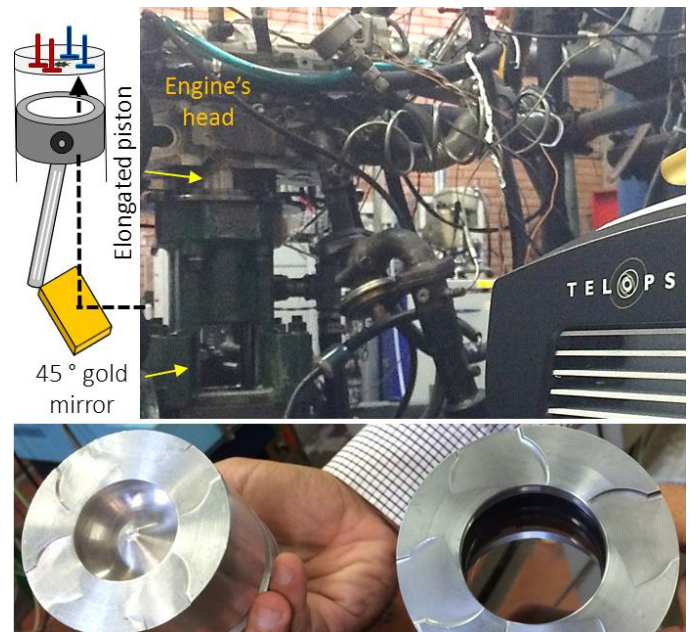


Figure 1 Infrared imaging carried out on the optical engine.

solve the problem of the pollutant emissions from a CI engine completely. For this reason, one alternative considered by researchers in this field consists in using a

dual-fuel configuration engine [1]. In dual-fuel CI engines, natural gas serves as the primary fuel while a “pilot” amount of liquid Diesel fuel is used as an ignition source. The gaseous fuel, i.e. methane ( $\text{CH}_4$ ), is inducted along with the intake air and undergoes compression just like in a conventional Diesel engine. The mixture of air and gaseous fuel does not autoignite as a result of the compression stroke due to its high autoignition temperature. Therefore, a small amount of liquid Diesel fuel is needed near the end of the compression stroke in order to ignite the gaseous mixture. Since Diesel fuel usually autoignites under these conditions, it creates ignition sources for the surrounding air–gaseous fuel mixture. The pilot liquid fuel, which is injected by the conventional Diesel injection equipment, normally contributes to only a small fraction of the engine power output [2].

Research activities on operating ICEs are very challenging as fast chemical reactions occur in a closed vessel, in high-temperature and high-pressure conditions. Characterization techniques must also account for changing physical and optical properties of the medium. Rapid phase transition, from liquid to the gas phase, occurs when liquid diesel fuel is injected in a high-temperature environment (cylinder containing pressurized gases). For these reasons, having access to a diagnostic tool allowing investigation under all these constraints represents an important asset. In this work, a modified diesel engine (see Figure 1) was used in combination with the Telops FAST-IR 2K, a high-performance cooled high-speed infrared camera, for investigation of the various cycles of a diesel ICE. The engine was operated in a dual-fuel configuration, i.e. air was replaced by a premixed methane-air charge. The various stages, i.e. intake, compression, diesel-fuel injection, working stroke and exhaust, were characterized at a frame rate of 26 KHz using different attenuation and spectral filters (broadband,  $\text{CO}_2$  red-spike, through-flame and hydrocarbon). The results illustrate the potential of high-speed IR imaging as a diagnostic tool for ICEs.

## Experimental Information

### Optical Engine

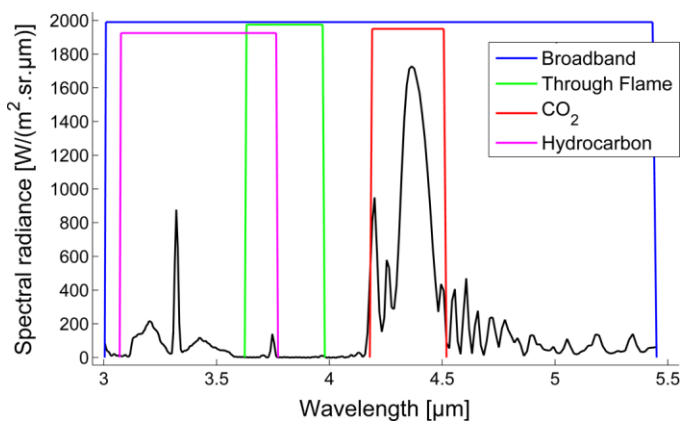
The optical engine is a single-cylinder engine equipped with the combustion system architecture and injection system of a commercial 4-cylinder diesel passenger’s car. In order to be able to carry out imaging of the combustion chamber while the engine is in operation, part of the piston crown was replaced by a 12-mm thick sapphire window, as shown in Figure 1. An elongated piston configuration is also used to make space for a 45° gold mirror in the cylinder’s axis. The elongated single-cylinder transparent engine has stroke and bore dimensions of 92 mm and 85 mm, respectively, and a compression ratio of 16.5:1. Commercial grade diesel fuel was used for all experiments, using a common rail injection system. The setup is equipped with a fully opened electronic control unit (ECU), which allows full control on diesel fuel injection and timing. In particular, for dual fuel operation, diesel fuel was injected directly into the cylinder at a mass flow rate of 0.400 kg/h under a pressure of 800 bar and at 6° crank angle before top dead center. This represents a small amount with respect to the same operating conditions realized by means of conventional diesel combustion. The production intake manifold of the engine was modified to set an electronic port fuel injector (PFI) generally used in modern engines. It was a production unit suitable for gaseous fuel. It was fed by an automotive electrical pump able to reach up to 5 bar of injection pressure and was used with methane fuel. The air and methane mass flow rate were set to 33.5 kg/h and 0.385 kg/h respectively. The engine’s revolution was set to 1500 revolution per minute (RPM).



Figure 2 The Telops FAST-IR 2K.

### High-Speed Infrared Imaging

The Telops FAST-IR 2K (Figure 2) is a cooled high-performance infrared camera using a 320×256-pixel indium antimonide (InSb) focal plane array (FPA) detector covering the 3–5.5 μm spectral range. A 50-mm Janos lens was used for all experiments. A 64×64 pixel sub-portion of the FPA detector was used for imaging at 26 000 frames per second. The total recording time was set to 1 sec for each measurement. The camera is equipped with a 4-position internal filter wheel that allows the storing of 1-inch (2.54 cm) infrared filters. The engine’s operation was investigated using a total of five different filters: optical density (OD) 1.0, OD 2.0, bandpass 3.80 ±0.18 μm, bandpass 4.35 ±0.18 μm and bandpass 3.42 ±0.35 μm. The spectral response of the different filters along with the spectral radiance spectrum of a typical methane combustion, measured by midwave infrared remote sensing, is shown in Figure 3.



**Figure 3 Typical spectral radiance associated with a methane combustion as well as the spectral range covered by the infrared spectral filters.**

Due to atmospheric absorption, the CO<sub>2</sub> spectral features appears like two separate peaks: the blue (4.15 μm) and the red spike (4.35 μm). For this reason, the bandpass 4.35 ±0.18 μm spectral filter is often referred to the CO<sub>2</sub> red-spike filter. There is almost no infrared self-emission contribution from major combustion products in the 3.6–4.0 μm spectral range. For this reason, the bandpass 3.80 ±0.18 μm filter is often referred to as being a through-flame filter. The 3.0–3.5 μm spectral range is typically associated with the C–H stretching vibration

spectral feature. As all hydrocarbons contain at least one C–H chemical bound, a bandpass 3.42 ±0.35 μm spectral filter is often referred to as being a hydrocarbon filter.

### Image Processing

At the engine’s revolution speed, 11 successive 4-stroke cycles were recorded for each measurement. Due to the high periodicity of the phenomena and great reproducibility for cycle to cycle, the median value associated with each crank angle was computed for each experiment. In the case of the broadband infrared sequence, a composite sequence was made by using data from both the experiment carried out with the OD 1.0 and the OD 2.0 attenuation filter in order to account for the large temperature dynamic range. In order to do so, the saturated pixels identified in the experiment carried out with the OD 1.0 were replaced with the corresponding pixels from the measurements carried out with the OD 2.0 filter. The atmospheric, sapphire window and gold mirror contributions were accounted for according to the following radiative transfer equation:

#### Equation 2

$$L_{\text{tot}} = \left( \left( L_{\text{comb}} \tau_{\text{saph}} + L_{\text{saph}} (1 - \tau_{\text{saph}}) \right) \tau_{\text{mir}} + (1 - \tau_{\text{mir}}) L_{\text{room}} \right) \tau_{\text{atm}} + (1 - \tau_{\text{atm}}) L_{\text{atm}}$$

where  $L_{\text{tot}}$  is the measured spectral radiance,  $L_{\text{comb}}$ , the spectral radiance associated with the combustion inside the chamber,  $\tau_{\text{saph}}$ , the transmittance of a 12-mm-thick sapphire window,  $L_{\text{saph}}$ , the self-emission associated with the sapphire window (estimated to 450 K),  $\tau_{\text{mir}}$ , the transmittance of unpolarised radiation on the gold mirror at 45° (derived from its reflectivity curve),  $L_{\text{room}}$ , the self-emission associated with the surroundings under ambient conditions,  $\tau_{\text{atm}}$ , the atmospheric transmittance, and  $L_{\text{atm}}$ , the self-emission associated with the atmosphere. Calculations consisted in estimating the temperature corresponding to the in-band radiance of a blackbody source in the spectral range associated with the selected filter.

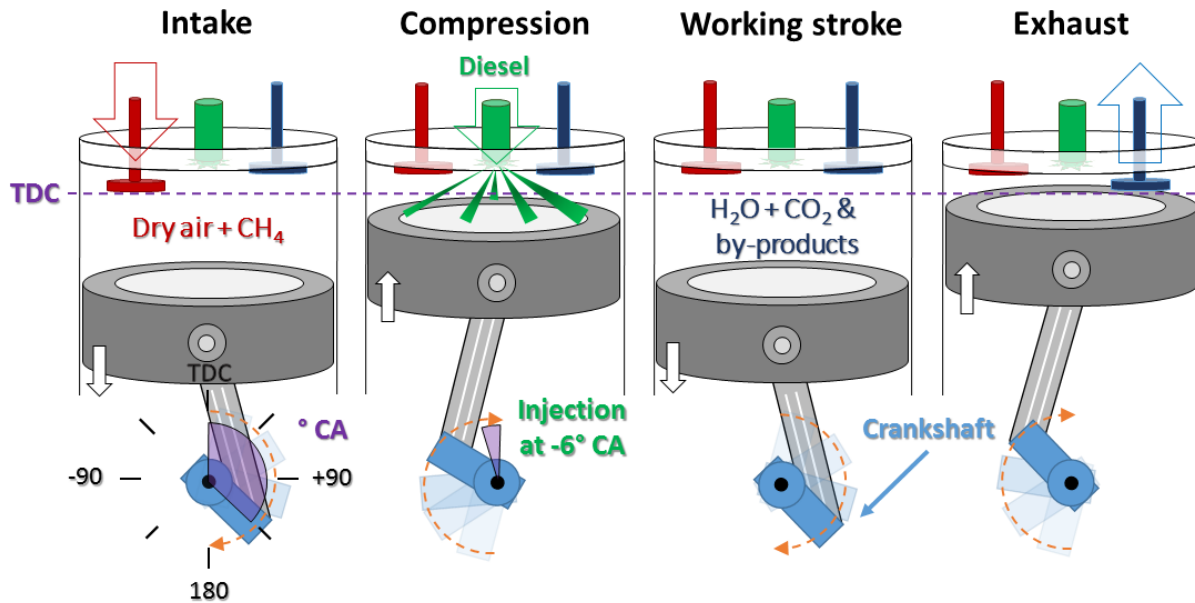


Figure 4 Schematic representation of a typical 4-cycle diesel internal combustion engine.

## Results and Discussion

### 4-cycle Diesel ICE

The main components of a conventional 4-stroke CI engine are illustrated in Figure 4. Intake and exhaust valves move upward and downward in order to close the cylinder or establish an access to it under the action of a camshaft (not shown). The injector is responsible for spraying the fuel into fine droplets to facilitate vaporization. The upward and downward motion of the piston assembly is translated into a gyration movement by means of a crankshaft. As a matter of fact, the engine’s reference frame is often expressed in terms of crank angle ( $^{\circ}$  CA) where the  $0^{\circ}$  CA position corresponds to the top dead centre (TDC) position. In the present work, the temporal resolution corresponds to  $0.35^{\circ}$  CA per frame. Detailed investigation of all four strokes and the liquid fuel injection of the diesel ICE is presented in the following sections.

### Intake Stroke

During the intake stroke, intake valves are fully opened while the piston is going downward ( $0-180^{\circ}$  CA) in order to fill the combustion bowl with a methane–dry air blend.

In the present experiment, both the dehumidified, heated up, and filtered air and gaseous fuel (i.e. CH<sub>4</sub>) enter the combustion chamber at the same time. The intake pressure was managed in order to achieve high air mass flow rate at fixed engine speed. A schematic view of the investigated region and a typical infrared image recorded during the intake stroke are presented in Figure 5.

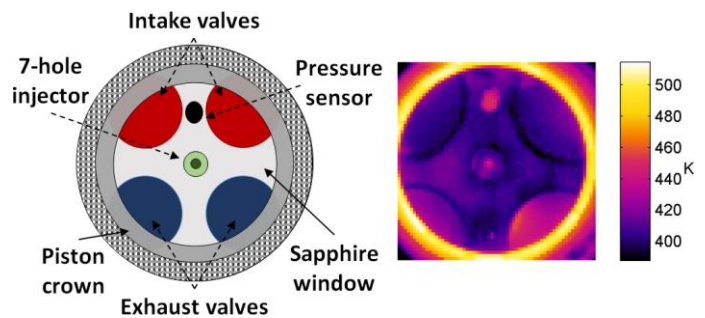


Figure 5 Schematic view (left) and infrared image (right) of the combustion chamber.

From an infrared imaging perspective, the intake stroke involves 2 infrared-active molecules; CO<sub>2</sub> from the compressed dry air and CH<sub>4</sub>. As their temperature is close to ambient temperature when exiting the PFI, weak thermal contrast associated with their presence is typically observed during measurements on intake strokes (data not shown).

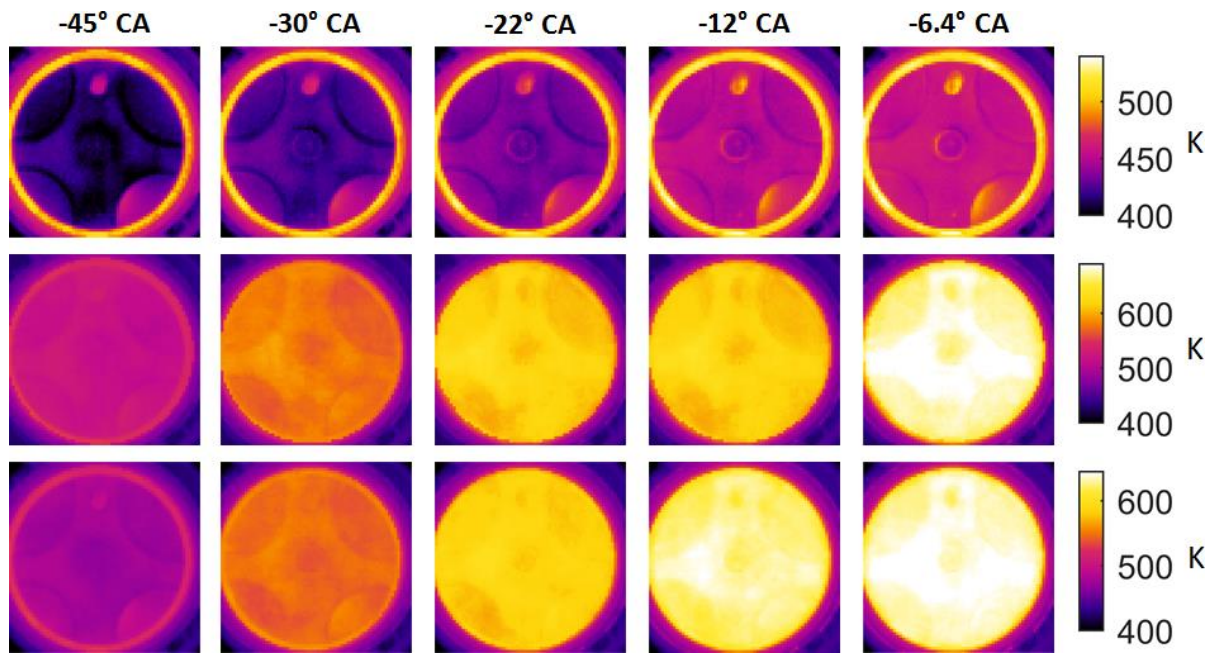


Figure 6 Various stages of the compression stroke seen through different infrared spectral bands.

### Compression Stroke

During the compression stroke, all valves are closed while the pressure gradually increases as a result of the upward motion of the piston and the compression ratio of the engine (180–0° CA). During the compression stroke, the mechanical work is not fully converted into a pressure increase as poor thermal exchanges are taking place between the system and its surrounding. Therefore, the gas temperature increases significantly as a result of nearly adiabatic compression, as shown in Figure 6. Since the charge contains both CO<sub>2</sub> (from the air) and CH<sub>4</sub>, the highest thermal contrast associated with adiabatic compression is seen through the CO<sub>2</sub> red-spike and hydrocarbon spectral filters. Since compression is not purely adiabatic, a weak temperature increase can still be seen in the through-flame spectral filter sequence as a result of grey-body self-emission from the different components. Sufficient temperature increase upon compression is critical for good

performance of CI engines since autoignition of diesel fuel only occurs beyond a certain temperature threshold.

It should be noted that the temperature reading of the same event observed under different spectral bands conditions do not correspond to actual thermodynamic temperature differences. The gas temperature appears differently as a function of wavelength due to the spectral absorption/emission features (see also Figure 3). The radiometric calibration of a MWIR camera is typically relative to a blackbody source, i.e. an object of constant spectral emissivity of one across all wavelengths. This temperature reference frame is somewhat incompatible with selective absorbers/emitters of infrared radiation like hot combustion gases. Nevertheless, the reported temperatures correspond to the in-band radiance of a blackbody source in the spectral range associated with the selected filter. Further flame simulation work (e.g., computer fluid dynamic [CFD]) is required in order to estimate the actual gas temperature from the infrared imaging measurements.

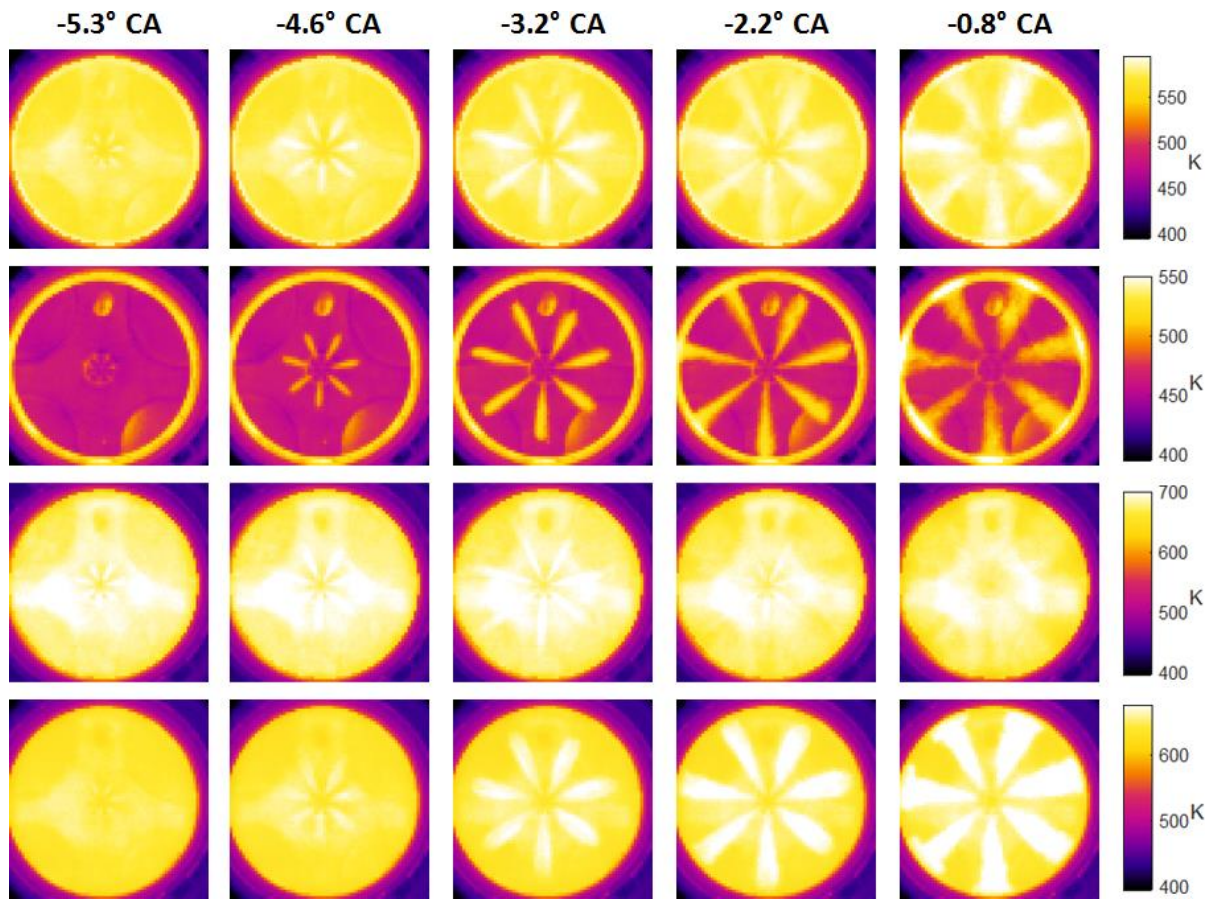


Figure 7 Various stages of the diesel fuel injection seen through different infrared spectral bands.

### Diesel Injection

While approaching TDC, the temperature in the combustion chamber increases more and more. At this stage ( $-6^\circ$  CA for these experiments), diesel fuel is injected into the combustion bowl under high-pressure conditions, as shown in Figure 7. In the early stage, diesel fuel is still in a liquid phase and behaves like a grey-body. Consequently, the greatest thermal contrasts associated with liquid fuel can be seen using both the broadband and through-flame channels. The highest contrast among all is observed using the through-flame spectral filter, since no contribution from the hot compressed  $\text{CO}_2$  and  $\text{CH}_4$  gases occurs in this spectral band. As the fuel vaporises, it starts behaving like a semi-translucent media with distinct absorption features. Diesel fuel is a mixture of saturated and branched carbon chains, with a few insaturations (e.g.,  $\text{C}_{16}\text{H}_{34}$ ). Therefore, each molecule contains many C–H chemical bounds, which are known

for depicting distinct spectral features in the  $3\text{--}3.5\ \mu\text{m}$  spectral range. For this reason, thermal contrasts associated with diesel fuel in the gas phase are better observed with the hydrocarbon spectral filter. A multipoint injector disperses the fuel in several directions to favor fuel mixing with air as it vaporizes. When looking at the 7-arm-star shape created by the 7-hole diesel fuel injector, it can be seen that the “arms” of the star are significantly larger in the sequence recorded with the hydrocarbon filter than the sequence recorded with the through-flame filter. This is mainly due to the lateral diffusion of gaseous diesel fuel as it vaporizes. As expected, this effect is more and more pronounced as a function of time as a result of the liquid–gas phase transition. As expected, very weak contrast associated with diesel fuel, in the liquid or gas phase, is observed in the  $\text{CO}_2$  bandpass filter other than its grey-body contribution in this spectral range.

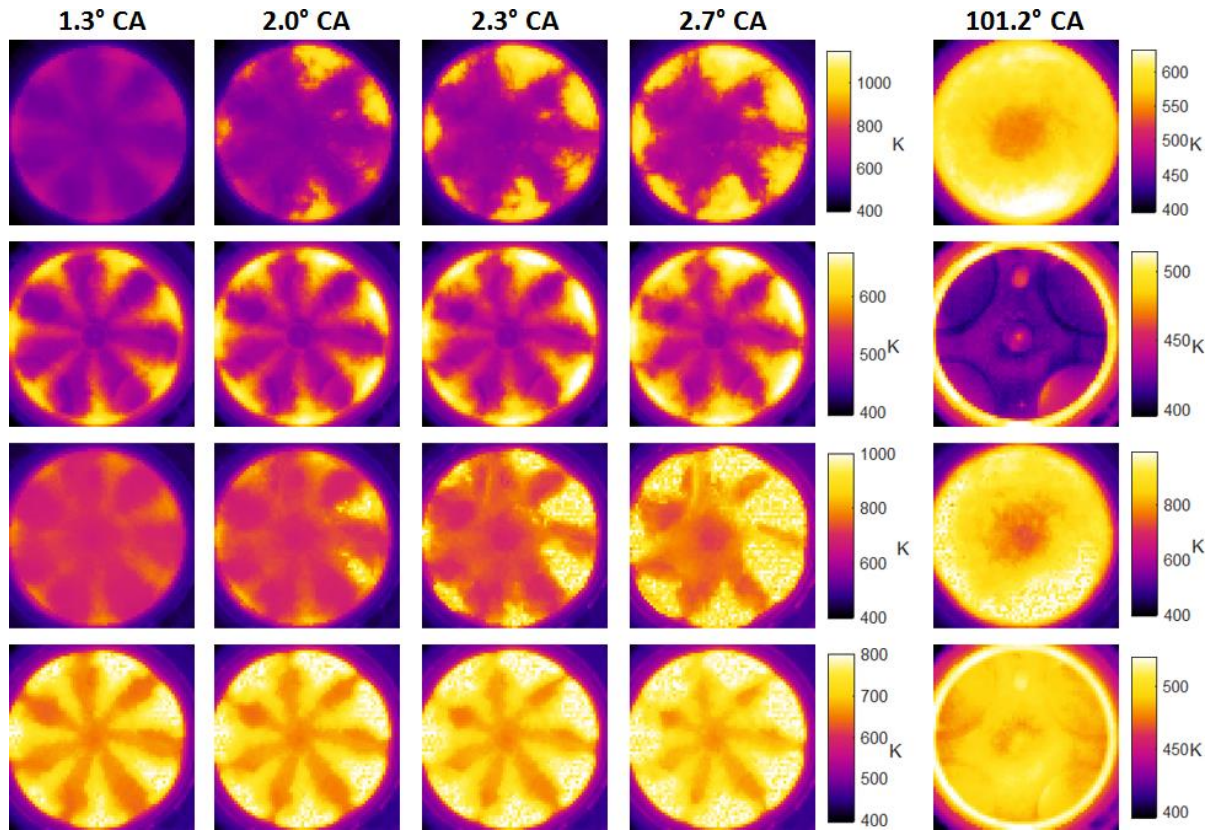
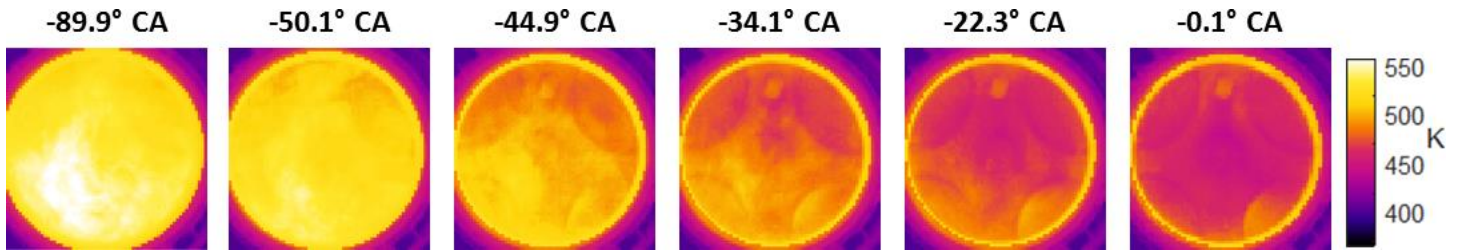


Figure 8 Various stages of the working stroke seen through different infrared spectral bands.

### Working Stroke

At some point, temperatures are sufficiently high so that the little amount of vaporized diesel fuel ignites spontaneously. This first ignition then serves as an ignition source for methane. In a dual-fuel configuration, diesel fuel acts as a pilot fuel as most of the engine's power comes from methane combustion. Four frames recorded at the early ignition stage are shown in Figure 8. can see that the ignition starts from the piston bowl wall, although the temperature of the compressed gas, prior to ignition, appears to be quite homogeneous. This likely illustrates the fact that diesel fuel first needs to vaporize sufficiently, then to mix with air, in high-temperatures conditions, for autoignition to occur. As seen in Figure 8, the flame rapidly propagates toward the center of the piston bowl in a few tens of microseconds. As combustion occurs, methane and diesel molecules are rapidly transformed into much greater amounts of gaseous CO<sub>2</sub> and H<sub>2</sub>O (see Equation 1). Since this large volume change takes place in a close vessel, this results

into a significant heat release and pressure increase. The remaining energy is converted into mechanical work to cause the downward motion of the piston (0–180° CA). The evolution of the chemical reaction can be followed by comparing the sequences recorded with the different spectral filters in Figure 8. In the regions where the thermal contrast associated with CO<sub>2</sub> increases, the thermal contrast associated with liquid fuel (through-flame) and hydrocarbons decreases at the same time. The last frames in Figure 8 correspond to a much later stage, about 55 %, of the working stroke. Nearly no trace from of the combustion gases can be seen in the image recorded with the through-flame filter, which is consistent with the spectral properties of a typical methane combustion (see Figure 3). Therefore, such spectral filters could be useful for temperature monitoring of critical engine parts like the injector, the valves and/or the pressure sensor during combustion. At this stage, most, but not necessarily all, of the diesel fuel and methane gas have been converted into CO<sub>2</sub> and water vapor. It is then not surprising to observe large



**Figure 9 Exhaust cycle investigated at various stages using the CO<sub>2</sub> red-spike spectral filter.**

thermal contrasts in the CO<sub>2</sub> red-spike filter at this point of the combustion cycle. Significant thermal contrast can still be observed in the infrared image recorded with the hydrocarbon spectral filter. It is not clear if this results from unburnt fuel, diesel and/or methane gas, water vapor or other byproducts such as partially oxidized hydrocarbons. Water vapor is a strong infrared emitter and has weak spectral features in the hydrocarbon filter spectral range. However, since water vapor is produced in large amounts in any hydrocarbon combustion (see Equation 1), its contribution cannot be totally discarded. Nevertheless, additional spectral information would be required to support these hypotheses. The signal recorded by broadband infrared imaging is in fact a sum of all contributions in the detector’s sensitivity range (3–5.5 μm in this case). Without spectral information, there is no way of knowing from what the signal originates. By comparing the frames recorded with different spectral bands, it is clear that the signal measured by broadband imaging is dominated by the CO<sub>2</sub> contribution.

**Exhaust Stroke**

During the exhaust stroke, exhaust valves are fully opened, while the piston is going upward (180 – 0° CA) in order to empty the cylinder before starting a new combustion cycle. Combustion gases exiting the combustion chamber through the two exhaust valves located in the lower part of the cylinder can be clearly seen in the sequence presented in Figure 9.

**Conclusion**

The different phases of a combustion cycle of a CI research engine operating in dual fuel mode could be

successfully investigated using high-speed infrared imaging. The use of multiple spectral filters allowed to see diesel fuel under both the liquid and gaseous phases as well as to highlight the presence other combustion gases. High-speed infrared imaging proves itself to be an interesting diagnostic tool for research aiming to improve diesel ICEs. In this regard, the dual-fuel configuration represents an interesting approach, as lowering the amount of soot particles could help slow down the clogging of after-treatment filters in the exhaust systems.

**Acknowledgments**

Telops would like to acknowledge the support of Ezio Mancaruso and Luigi Sequino from Istituto Motori Consiglio Nazionale delle Ricerche (CNR) in this work.

**References**

[1] Korakianitis, T., et al., “Natural-Gas Fueled Spark-Ignition (SI) and Compression-Ignition (CI) Engine Performance and Emissions” *Prog. Energy Combust. Sci.* **37** (2011) 89-112.  
 [2] Papagiannakis, R.G., et al., “Combustion and Exhaust Emission Characteristics of a Dual Fuel Compression Ignition Engine Operated with Pilot Diesel Fuel and Natural Gas” *Energy Conversion and Management* **45** (2004) 2971–2987.

**Telops Inc.**

100-2600 St-Jean Baptiste Ave  
 Québec, QC, Canada  
 G2E 6J5

Tel.: +1-418-864-7808  
 Fax. : +1-418-864-7843  
[sales@telops.com](mailto:sales@telops.com)  
[www.telops.com](http://www.telops.com)